

# Nuclear Theory – Nuclear astrophysics

J.W. Holt

## I. Introduction

The structure, phases, and dynamics of nuclear matter are crucial to understand stellar explosions, the origin of the elements, patterns in observed gravitational waves, and the composition of the densest observable matter in the universe. The appropriate tool to study strongly interacting matter at the typical scales relevant in nuclear astrophysics (well below the scale of chiral symmetry breaking  $\Lambda\chi\approx 1$  GeV) is chiral effective field theory [1-3]. In recent years, chiral effective field theory has become a cornerstone of the modern approach to nuclear many-body dynamics that provides a systematic framework for describing realistic microphysics, such as multi-pion exchange processes and three-body forces, within a well-defined organizational hierarchy. The long and intermediate-range parts of the nuclear potential result from one- and two-pion exchange processes, while short-distance dynamics, not resolved at the wavelengths corresponding to typical nuclear Fermi momenta, are introduced as contact interactions between nucleons. Chiral effective field theory is unique in its multichannel methods for quantifying uncertainties and especially in its ability to estimate the importance of missing physics.

## II. Neutrino reactions in warm, neutron-rich matter

Neutrinos dominate the transport of energy, momentum, and lepton number in extreme astrophysical settings, such as core-collapse supernovae [4,5], newly born neutron stars [6,7], and neutron star mergers [8,9]. Both neutral-current elastic scattering processes and charged-current absorption processes affect the total neutrino and anti-neutrino opacities in these environments. In a dense medium, the free-space elastic scattering and absorption cross sections are modified due to nuclear mean fields and correlations. These effects are encoded in dynamical structure functions that can be obtained from the imaginary part of nuclear response functions. Previously, nuclear matter response functions have been studied using a variety of nuclear interactions and many-body approximations, including nonrelativistic and relativistic mean field models [10,11], Fermi liquid theory [12,13], the virial expansion [14]. Recent studies [15,16] have highlighted the important role of nuclear mean fields for calculating charged-current reactions in the supernova neutrinosphere. Here the large asymmetry between proton and neutron densities leads to a strong splitting of the proton and neutron mean fields that enhances neutrino absorption and suppresses anti-neutrino absorption. This, in turn, affects the composition of matter ejected from supernovae and neutron star mergers as well as neutrino flavor and energy distributions that terrestrial neutrino detectors may observe.

In recent work [17], we have employed nuclear forces based on chiral effective field theory to investigate beyond-mean-field corrections to spin and density response functions of nuclear matter under ambient conditions typical of supernova and neutron star merger neutrino-spheres, where the nucleon number density varies in the range  $0.001 n_0 < n < 0.1 n_0$ , with  $n_0 = 0.16 \text{ fm}^{-3}$  the nuclear matter saturation density, and the temperature varies in the range  $5 \text{ MeV} < T < 10 \text{ MeV}$ . Specifically, we calculated Hartree-

Fock mean field corrections as well as re-summed particle-hole vertex corrections in the random phase approximation (RPA). In Fig. 1 we show the inverse mean free paths for electron neutrino (blue) and

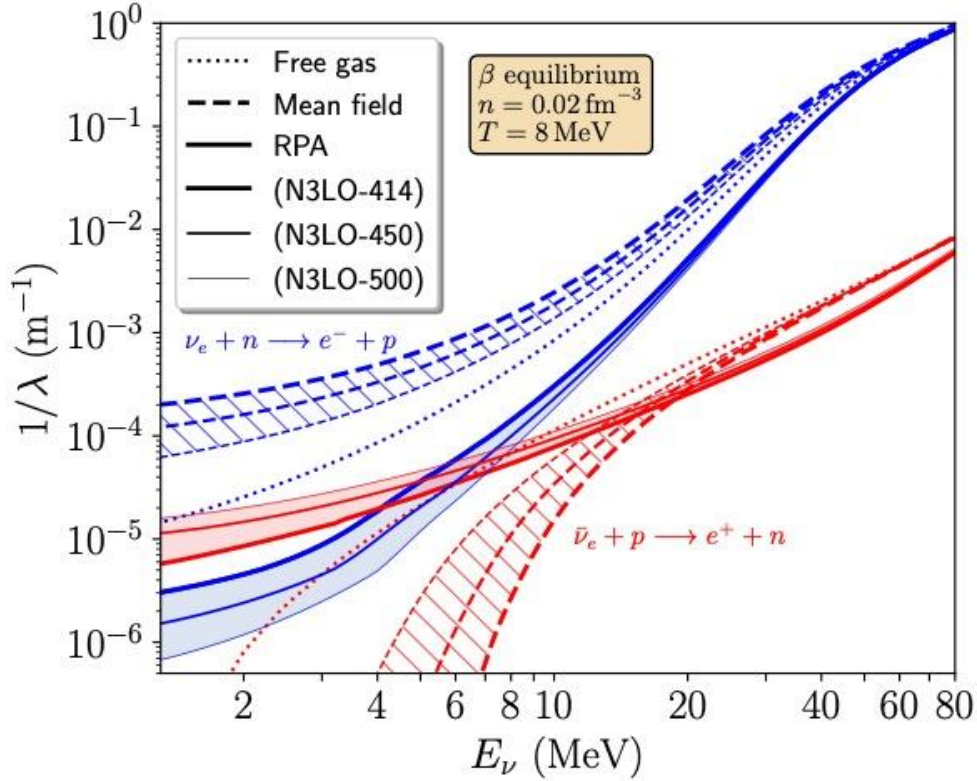


FIG. 1. Electron neutrino (blue) and antineutrino (red) inverse mean free paths as a function of energy for beta-equilibrium nuclear matter at density  $n = 0.02 \text{ fm}^{-3}$  and temperature  $T = 8 \text{ MeV}$ . The dotted lines denote results for noninteracting nucleons, the dashed curves denote results including nuclear mean fields at the Hartree-Fock level, and solid lines represent results including both mean fields and random phase approximation vertex corrections. The shaded bands denote uncertainties due to the choice of nucleon-nucleon potential.

antineutrino (red) absorption as a function of the incident energy for beta-equilibrium nuclear matter at density  $n = 0.02 \text{ fm}^{-3}$  and temperature  $T = 8 \text{ MeV}$ . The dynamic structure functions are computed from the associated charged-current spin response functions in three approximations. First, the inverse neutrino mean free paths neglecting interactions between nucleons are shown by the dotted curves. Second, we show as the dashed lines the effect of introducing proton and neutron mean fields in the Hartree-Fock approximation. Finally, the solid curves show the combined effects of nucleon mean fields and vertex corrections obtained in the random phase approximation. We employ three different chiral nucleon-nucleon interactions: N3LO-414, N3LO-450, and N3LO-500.

In all cases, we find that the mean-field effects significantly enhance the electron neutrino absorption cross-section and suppress the electron antineutrino absorption cross-section across all energies considered, in agreement with previously published studies. The effects are largest for the most perturbative chiral potential, N3LO-414. In contrast, RPA correlations redistribute strength to the vicinity of a positive-energy collective mode. This significantly reduces the outgoing electron energy into a region where Pauli

blocking suppresses the reaction. This redistribution of strength due to a broad collective mode shifts the response to higher energy and undoes the enhancement of the inverse mean free path due to mean-field effects. Remarkably, correlations suppress the electron neutrino absorption cross-sections over the entire energy range and are especially large for low-energy neutrinos. Whereas the inclusion of nuclear mean fields resulted in a clear splitting of the electron neutrino absorption cross section with varying nuclear potential, the fact that the order and relative magnitude of the splitting remains intact after the inclusion of RPA correlations suggests these effects are less sensitive to the choice of NN potential. In particular, RPA correlations suppress the inverse mean free path by approximately two orders of magnitude for all three chiral potentials.

### III. Generative modeling of the nucleon-nucleon interaction

Developing high-precision models of the nuclear force and propagating the associated uncertainties in quantum many-body calculations of nuclei and nuclear matter remain key challenges for ab initio nuclear theory. In recent work [18], we have demonstrated that generative machine learning models, specifically the Generative Flow (“Glow”) model, can construct novel instances of the nucleon-nucleon interaction when trained on existing potentials from the literature. In particular, we modified and trained the Glow model on nucleon-nucleon potentials derived at second and third order in chiral effective field theory and at three different choices of the resolution scale. We then showed that the model can be used to generate samples of the nucleon-nucleon potential drawn from a continuous distribution in the resolution-scale parameter space. This work provides an important step toward a comprehensive estimation of theoretical uncertainties in nuclear many-body calculations that arise from the arbitrary choice of nuclear interaction and resolution scale.

In Fig. 2 we show neutron-proton scattering phase shifts in selected partial-wave channels ( $1S_0$ ,  $3S_1$ ,  $3P_0$ ,  $3P_1$ ,  $3P_2$ ,  $1D_2$ ,  $3D_1$ ,  $3D_2$ ,  $3D_3$ ) predicted from nuclear potentials generated by the Glow model. The samples are generated over a continuum of resolution scales defined by the value of the cutoff scale  $\Lambda$

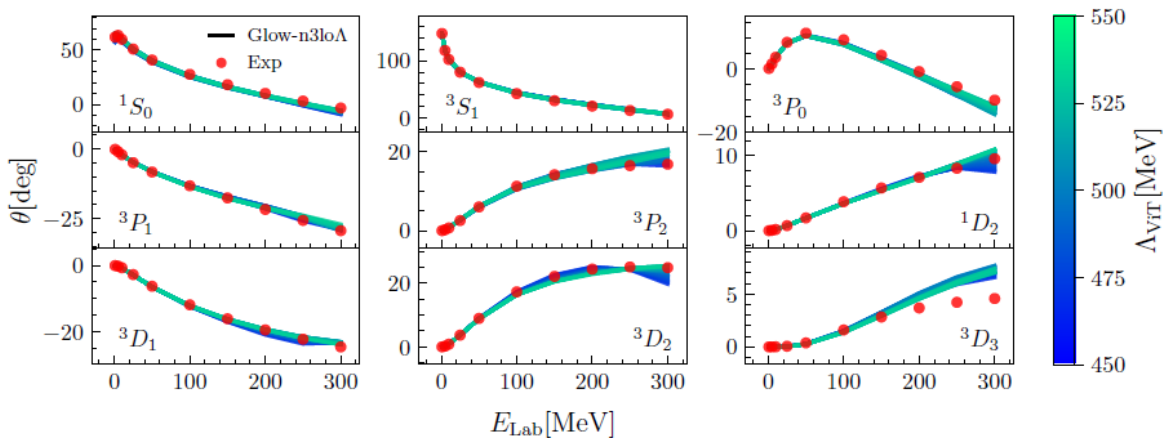


FIG. 2. Neutron-proton scattering phase shifts in selected partial-wave channels computed from Glow-generated nuclear potentials. The colors of the solid lines represent the values of the high-momentum cutoff  $\Lambda$ , which can take on a continuum of values. The red dots correspond to the phase shift analysis of nucleon-nucleon scattering data in [19].

used to regulate the high-momentum components of the nucleon-nucleon potential. The red dots correspond to the phase shift analysis in Ref. [19]. One sees that the Glow model is capable of generating realistic nucleon-nucleon potentials that produce high-quality scattering phase shifts. One can also observe that although the potentials are generated uniformly over the interval  $450 \text{ MeV} < \Lambda < 550 \text{ MeV}$ , the associated phase shift values are not uniformly distributed. This indicates the presence of complicated correlations between  $\Lambda$  and observables, highlighting the need for general statistical uncertainty analysis tools that are presently unavailable in the literature.

- [1] S. Weinberg, *Physica A* **96**, 327 (1979).
- [2] E. Epelbaum, H.-W. Hammer and U.-G. Meissner, *Rev. Mod. Phys.* **81**, 1773 (2009).
- [3] R. Machleidt and D. R. Entem, *Phys. Rep.* **503**, 1 (2011).
- [4] A. Burrows and R. F. Sawyer, *Phys. Rev. C* **59**, 510 (1999).
- [5] T. Melson, H.-T. Janka, R. Bollig, F. Hanke, A. Marek, and B. Mueller, *Astrophys. J. Lett.* **808**, L42 (2015).
- [6] J.A. Pons, S. Reddy, M. Prakash, J.M. Lattimer, and J.A. Miralles, *Astrophys. J.* **513**, 780 (1999).
- [7] L.F. Roberts and S. Reddy, *Phys. Rev. C* **95**, 045807 (2017).
- [8] Y. Sekiguchi, *Class. Quant. Grav.* **27**, 114107 (2010).
- [9] S. Wanajo, Y. Sekiguchi, N. Nishimura, K. Kiuchi, K. Kyutoku, and M. Shibata, *Astrophys. J. Lett.* **789**, L39 (2014).
- [10] R.F. Sawyer, *Phys. Rev. C* **40**, 865 (1989).
- [11] S. Reddy, M. Prakash, and J.M. Lattimer, *Phys. Rev. C* **58**, 013009 (1998).
- [12] N. Iwamoto and C.J. Pethick, *Phys. Rev. D* **25**, 313 (1982).
- [13] A. Burrows and R.F. Sawyer, *Phys. Rev. C* **58**, 554 (1998).
- [14] C.J. Horowitz and A. Schwenk, *Phys. Lett. B* **642**, 326 (2006).
- [15] G. Martinez-Pinedo, T. Fischer, A. Lohs, and L. Huther, *Phys. Rev. Lett.* **109**, 251104 (2012).
- [16] L.F. Roberts, S. Reddy, and G. Shen, *Phys. Rev. C* **86**, 065803 (2012).
- [17] E. Shin, E. Rrapaj, J.W. Holt and S.K. Reddy, *Phys. Rev. C* **109**, 015804 (2024).
- [18] P. Wen, J.W. Holt and M. Li, arXiv:2306.13007.
- [19] R. Navarro Prez, J.E. Amaro, and E. Ruiz Arriola, *Phys. Rev. C* **89**, 064006 (2014).